

See discussions, stats, and author profiles for this publication at: <https://www.researchgate.net/publication/45404914>

# Transition between B-DNA and Z-DNA: Free energy landscape for the B-Z junction propagation

ARTICLE *in* THE JOURNAL OF PHYSICAL CHEMISTRY B · AUGUST 2010

Impact Factor: 3.3 · DOI: 10.1021/jp103419t · Source: PubMed

---

CITATIONS

11

READS

54

## 4 AUTHORS, INCLUDING:



Juyong Lee

National Institutes of Health

23 PUBLICATIONS 161 CITATIONS

[SEE PROFILE](#)

## Transition between B-DNA and Z-DNA: Free Energy Landscape for the B-Z Junction Propagation

Juyong Lee,<sup>†</sup> Yang-Gyun Kim,<sup>‡</sup> Kyeong Kyu Kim,<sup>§</sup> and Chaok Seok\*,<sup>†</sup>

Department of Chemistry, Seoul National University, Seoul 151-747, Korea, Department of Chemistry, Sungkyunkwan University, Suwon 440-746, Korea, and Department of Molecular Cell Biology, Sungkyunkwan University School of Medicine, Suwon 440-746, Korea

Received: April 16, 2010; Revised Manuscript Received: May 31, 2010

Canonical, right-handed B-DNA can be transformed into noncanonical, left-handed Z-DNA in vitro at high salt concentrations or in vivo under physiological conditions. The molecular mechanism of this drastic conformational transition is still unknown despite numerous studies. Inspired by the crystal structure of a B-Z junction and the previous zipper model, we show here, with the aid of molecular dynamics simulations, that a stepwise propagation of a B-Z junction is a highly probable pathway for the B-Z transition. In this paper, the movement of a B-Z junction by a two-base-pair step in a double-strand nonamer, [d(GpCpGpCpGpCpG)]<sub>2</sub>, is considered. Targeted molecular dynamics simulations and umbrella sampling for this transition resulted in a transition pathway with a free energy barrier of 13 kcal/mol. This barrier is much more favorable than those obtained from previous atomistic simulations that lead to concerted transitions of the whole strands. The free energy difference between B-DNA and Z-DNA evaluated from our simulation is 0.9 kcal/mol per dinucleotide unit, which is consistent with previous experiments. The current computation thus strongly supports the proposal that the B-Z transition involves a relatively fast extension of B-DNA or Z-DNA by sequential propagation of B-Z junctions once nucleation of junctions is established.

### Introduction

The first crystal structure of DNA determined in 1979 was a noncanonical, left-handed double helical form of DNA, Z-DNA.<sup>1</sup> It was later revealed that Z-DNA is not just an abnormal species of DNA but plays several important physiological roles in living organisms. A high density of Z-DNA favoring base sequences, purine-pyrimidine alternations, exists near transcription start sites,<sup>2</sup> and formation of Z-DNA induced by Z-DNA binding proteins near the promoter region boosts transcription of the downstream genes.<sup>3</sup> It is now thought that Z-DNA formation is closely related to the regulation of gene expression, DNA processing events, and genetic instability.<sup>4,5</sup>

It is well-known that B-DNA undergoes spontaneous and reversible transition to Z-DNA under conditions of high ionic strength, for example in 4 M NaCl solution,<sup>6</sup> or upon binding of Z-DNA binding proteins.<sup>3,7</sup> However, the manner in which the radical structural change from B-DNA to Z-DNA and vice versa is accomplished at the atomic level is still unknown. A popular model for the B-Z transition is the zipper model, which suggests that the transition is initiated by the formation of two B-Z junctions and followed by stepwise propagation of the junctions in opposite directions of the double helix.<sup>8–11</sup> The zipper model was successful in explaining gradual changes in the mobility of cyclic DNAs in 2-D gel electrophoresis experiments under different negative superhelical stresses,<sup>8</sup> but what structural changes are involved in the transition is not known yet at the atomic level.

A number of molecular mechanisms have been proposed to explain the change in the handedness of DNA double helix and the 180° base-pair plane rotation during the B-Z transition, including the Wang model,<sup>1</sup> the Harvey model,<sup>12</sup> the A-DNA-like intermediate model,<sup>13</sup> and the model based on the crystal structure of a B-Z junction.<sup>14</sup> The Wang model proposes that base-pair opening occurs before base-pair plane and phosphate backbone angle rotation.<sup>1</sup> The Harvey model suggests that the B-Z transition takes place through flipping of base-pair planes pair by pair without disruption of the Watson-Crick (WC) base-pairing.<sup>12</sup> The A-DNA-like intermediate model postulates that the transition occurs through an A-DNA-like intermediate without breaking of base-pairing or severe steric hindrance.<sup>13</sup> Finally, extrusion of bases, as observed in the crystal structure of a B-Z junction, was proposed to occur and to propagate by reformation of base pairs.<sup>14</sup> These mechanisms were proposed based on structural differences between B- and Z-DNA, but the feasibilities of such transition pathways have not been fully justified in terms of the energetics involved in the proposed structural changes.

By virtue of recent advances in molecular dynamics (MD) simulation technologies and nucleic acids force fields, the mechanism of the B-Z transition has been tackled with realistic all-atom simulations by several authors. The B-Z transition pathway for a heptamer duplex, [d(GpCpGpCpGpCpG)]<sub>2</sub>, under an implicit solvent environment was investigated<sup>15</sup> with the stochastic difference equation (SDE) algorithm, which finds the minimum potential path based on the minimum action principle.<sup>16</sup> A targeted molecular dynamics simulation method (TMD)<sup>17</sup> was also employed to study the pathway of the B-Z transition of a hexamer, [d(GpCpGpCpGpC)]<sub>2</sub>, in an explicit water environment, and the potential of mean force of the transition was evaluated by integration of the driving force.<sup>18</sup>

\* To whom correspondence should be addressed. E-mail: chaok@snu.ac.kr.  
Phone: 82-2-880-9197. Fax: 82-2-871-8119.

<sup>†</sup> Seoul National University.

<sup>‡</sup> Sungkyunkwan University.

<sup>§</sup> Sungkyunkwan University School of Medicine.

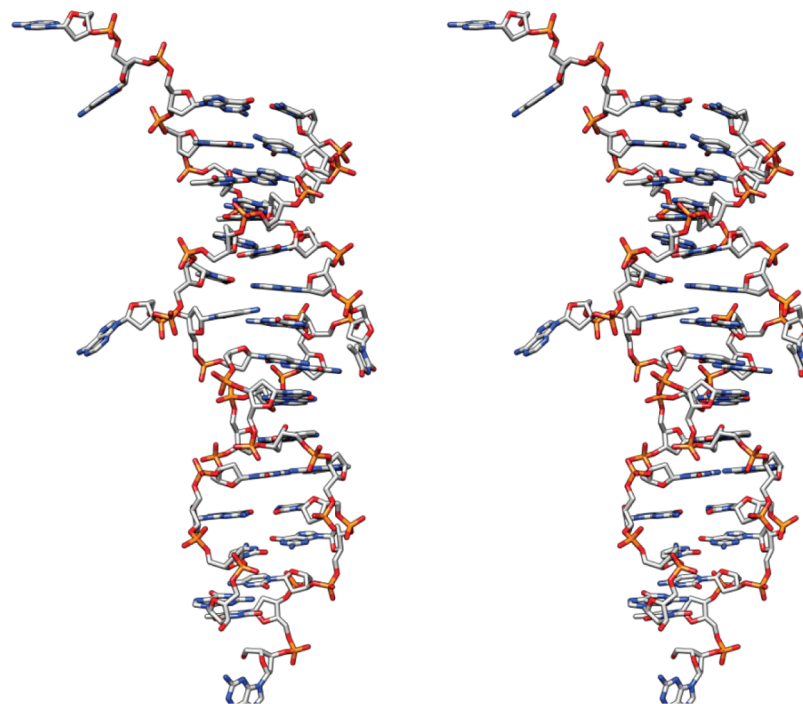


**Figure 1.** Stereo view of the crystal structure of a B-Z junction-containing DNA. Four Z-DNA binding proteins were stripped from the Z-DNA region. Except for the unpaired nucleotides at terminals, the top six base pairs conform to the B-DNA structure, the bottom eight base pairs conform to the Z-DNA structure, and one pair in between is extruded. With only single-base-pair extrusion, the dramatic reversal of the double helix handedness is accomplished.

A common feature of the transition pathways obtained from those simulations is that the B-Z transition occurs through a stretched intermediate state in a concerted manner. Stretching and parallelization of the phosphate backbone provides enough room for base rotation and a route for backbone rewinding in the opposite direction. In the simulated pathways backbone stretching and base-pair breaking of the entire DNA occurs simultaneously, although asynchronous base flipping was also reported.<sup>18</sup> The potential energy barrier of the transition, ~100 kcal/mol,<sup>15</sup> and the free energy barrier, ~30 kcal/mol,<sup>18</sup> are rather high, but may explain the spontaneous and reversible transition on a time scale of seconds to minutes in Z-DNA favoring environments.

The transition considered here is the B-Z junction propagation by a two-base-pair step. The end points of the transition were carefully designed based on the experimental structure of a B-Z junction. Two B-Z junctions form when a Z-DNA segment forms within a B-DNA chain, for example upon binding of Z-DNA binding proteins or under negative superhelical stress. The crystal structure of a B-Z junction determined in 2005<sup>14</sup> revealed that the dramatic change of handedness along a DNA chain can be achieved by extrusion of only a single base pair (See Figure 1). The cocrystallized four Z-DNA binding proteins stabilize the base pairs of Z-DNA, but do not interact with the extruded base pairs. The nucleotide pairs adjacent to the extruded bases show only slight deviation from the canonical B- or Z-DNA structure. This “static” B-Z junction may not necessarily correspond to the “dynamic” B-Z junction that was proposed to appear during the B-Z transition in the zipper model.<sup>8,11</sup> However, the surprisingly simple structure of the static B-Z junction inspired us to hypothesize that such junctions form dynamically and propagate sequentially along the chain during the B-Z transition.

The simplest B-Z junction propagation conceivable is the movement by two nucleotide pairs, the smallest repeating unit

of Z-DNA, increasing the length of B- or Z-DNA by two base pairs. A dinucleotide pair was also considered as a unit of the zipper model in previous studies.<sup>8,11</sup> Previous experimental reports that the length of a B-Z junction that appears in dynamic B-Z transitions is three base pairs or less support our hypothesis.<sup>19,20</sup> Successive movements of a B-Z junction can lead to the full B-Z transition by limiting structural perturbation to the smallest possible region at each transition step. This stepwise transition can provide a lower free energy barrier than a concerted transition that requires simultaneous breaking of multiple WC base pairs and deformation of the entire backbone. For a concerted transition, the barrier of the transition is expected to increase linearly with the length of the DNA that undergoes transition, leading to an exponential slow down of the transition. A stepwise transition does not suffer from such a problem.

In this paper, a GC-repeat nonamer is considered, to compare the simulation results with previous experiments and simulations on GC-repeat oligomers and to realize the junction movement in the shortest possible DNA fragment. A transition between the two DNA states with the junction position shifted by two base pairs is considered. Targeted molecular dynamics (TMD) simulations<sup>17</sup> were first performed to obtain the initial points for subsequent umbrella sampling<sup>21</sup> along the transition pathway in the  $\Delta\text{rmsd}$  coordinate.<sup>22</sup> The potential of mean force, PMF, was computed with WHAM (Weighted Histogram Analysis Method).<sup>23</sup> This simulation study provides a realistic atomic level explanation of the B-Z transition pathway with thermodynamic and kinetic projections consistent with experimental data.

## Methods

**Molecular Dynamics Simulations of the Two End Points of the B-Z Junction Propagation.** In the present study, we consider a double-strand nonamer,  $[d(GpCpGpCpGpCpG)]_2$ , to investigate the B-Z junction movement as an

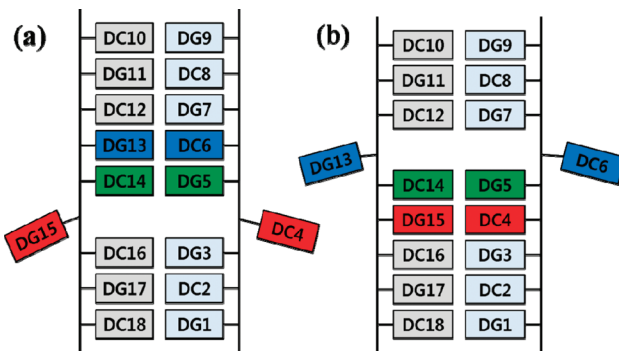


**Figure 2.** Schematic representations of the two end points for which simulations were performed for 5BJ3Z (a) and 3BJ5Z (b). The upper nucleotides in the figures represent those in the B-DNA conformation and the lower nucleotides those in the Z-DNA conformation. The three base pairs near the junction which suffer large conformational changes during the simulations are shown in red, green, and blue.

elementary step in the B-Z transition. Schematic pictures for the two end points of the transition, in which the position of the B-Z junction is shifted by two base pairs, are shown in Figure 2, together with notations for nucleotides. One end point of the transition shown in Figure 2a has five nucleotide pairs of B-DNA, three pairs of Z-DNA, and one extruded pair in between and is denoted by “5BJ3Z”. The other end point shown in Figure 2b has three and five nucleotide pairs of B- and Z-DNA, respectively, and an extruded pair in between and is denoted by “3BJ5Z”.

The initial structures for simulations of the two end points were built from the crystal structure<sup>14</sup> of a B-Z junction (RCSB PDB ID 2ACJ), which consists of 15 nucleotide pairs: 6 pairs in the B-form, 8 pairs in the Z-form, and one pair in between extruded out. All adenine and thymine bases in the B-DNA region were substituted by guanine and cytosine, keeping the relative orientations of the bases. Although the DNA structure depends on the base sequence in general, we expect that the B-Z junction of the GC repeat considered here adopts a structure close to the crystal B-Z junction structure, considering that there is no sequence-specific feature in the geometry of the crystal junction. The extruded bases do not make any base-specific interactions with the rest of the DNA, and base-pair stacking of other bases is well-conserved after base substitutions. In addition, there are many examples in which G-C pairs adopt the B-DNA structure and A-T pairs inserted in G-C repeats adopt the Z-DNA structure.<sup>11,24-27</sup> The geometries of the substituted bases were constructed according to the parameters and topologies defined in the AMBER99 force field<sup>28,29</sup> with the LEAP program of AMBER9.<sup>30</sup> The initial structures constructed this way remained stable for 3 ns MD simulations, as discussed in the Results and Discussion section.

MD simulation was performed for each end point, 5BJ3Z and 3BJ5Z, with the SANDER program of AMBER9. The AMBER99 force field and TIP3P<sup>31</sup> were employed to describe the energetics of the DNA and water, respectively. Sodium and chloride ions were added to neutralize the system and to simulate a salt concentration of 0.1 M. The total number of atoms in the system was 7998: 567 atoms in the DNA, 24 sodium ions, 6 chloride ions, and 2467 water molecules. The truncated octahedron periodic boundary condition and the Particle Mesh Ewald method<sup>32</sup> with 10 Å cutoff were applied to take account of the long-range electrostatic interactions. The SHAKE constraint,<sup>33</sup> which enables the use of a 2 fs time step, was employed in all simulations.

The initial models for 3BJ5Z and 5BJ3Z constructed by LEAP were subject to minimization with positional restraints on DNA followed by minimization of the entire system without restraint. The systems were then slowly heated to 300 K for 100 ps at constant volume. The Langevin temperature control with 1.0 ps<sup>-1</sup> collision frequency was applied. Isothermal-isobaric ensemble MD simulations for 200 ps then followed, to allow density adjustment at 1 atm with 1 ps of pressure relaxation time. Finally, NPT molecular dynamics simulations were carried out for 3 ns. The last snapshots of the two 3 ns simulations were used as the reference structures for the subsequent TMD simulations.

**Targeted Molecular Dynamics Simulations.** The B-Z transition is known to take from seconds to minutes, which is not accessible with current computational power. We therefore employed the targeted molecular dynamics simulation method<sup>17</sup> to obtain starting conformations for the subsequent umbrella sampling by accelerating the transition. The functional form of the restraining potential for a conformation  $\mathbf{x}$  at time  $t$  is given by

$$W(\mathbf{x}, t) = \frac{1}{2}Nk_T[R(\mathbf{x}) - R_{\text{tgt}}(t)]^2$$

where  $N$  is the number of atoms influenced by the restraining potential,  $k_T$  is the force constant per atom,  $R(\mathbf{x})$  is the rmsd of the conformation  $\mathbf{x}$  from the reference structure, and  $R_{\text{tgt}}(t)$  is the target rmsd value that decreases to zero linearly with time to drive the system from an initial state to the reference state. All the heavy atoms in DNA were subject to the restraining potential, and the force constant was set to 10.0 kcal/mol per atom.

The first TMD simulation was performed to drive the transition from 5BJ3Z to 3BJ5Z taking 3BJ5Z as the reference conformation. The target rmsd,  $R_{\text{tgt}}(t)$ , was set to 7.18 Å at  $t = 0$ , the initial rmsd of 5BJ3Z from 3BJ5Z, and linearly reduced to zero for a period of 10 ns. The second TMD was carried out in the opposite direction, starting from 3BJ5Z toward the midpoint of the TMD trajectory of the 5BJ3Z to 3BJ5Z transition for 6.5 ns. The midpoint of the transition is defined as the point at which the difference between the rmsds from the two end points is closest to zero. We performed TMD in this bidirectional fashion in order to obtain good sampling at both end points of the transition since TMD generally leads to poor convergence toward the target structure due to thermal fluctuations.<sup>17</sup>

**Umbrella Sampling and the Potential of Mean Force.** Starting from the trajectory obtained from the TMD simulations, the potential of mean force of the transition was evaluated by the umbrella sampling technique<sup>25</sup> and the WHAM analysis.<sup>27</sup> In umbrella sampling it is critical to select a proper reaction coordinate, and in the present study we employed the difference of the rmsd values,  $\Delta\text{rmsd}$ , from the two end point reference structures to describe the complex transformation effectively. rmsd from a single reference structure is a convenient reaction coordinate for a complex transition that involves many degrees of freedom because it is not trivial to pick up a single structural variable that effectively describes the whole complex transition. However, the hyper-volume in the conformational space increases with rmsd, resulting in a bias in the free energy, stabilizing states that correspond to large rmsd. In the  $\Delta\text{rmsd}$  coordinate, the extents of the hyper-volume toward the two reference points are at least symmetric. The use of  $\Delta\text{rmsd}$  as a reaction coordinate was first suggested in the calculation of the free energy profile of A- to B-DNA transition.<sup>26</sup>

The functional form of the restraining potential for conformation  $\mathbf{x}$  for the  $i$ th window in the current umbrella sampling is

$$W_i(\mathbf{x}) = \frac{1}{2} N k_U [\Delta R(\mathbf{x}) - R_{\text{tgt},i}]^2$$

where  $N$  is the number of heavy atoms of DNA,  $k_U$  is the force constant per atom,  $\Delta R(\mathbf{x})$  is the difference between rmsds from the two end point reference structures 5BJ3Z and 3BJ5Z,  $\Delta R(\mathbf{x}) = \text{rmsd}_{\text{5BJ3Z}}(\mathbf{x}) - \text{rmsd}_{\text{3BJ5Z}}(\mathbf{x})$ , and  $R_{\text{tgt},i}$  is the target  $\Delta\text{rmsd}$  value for the  $i$ th window, which corresponds to the minimum of the restraining potential at the window. Use of a restraining potential that involves  $\Delta\text{rmsd}$  is not available in the AMBER9 package, so the parallel version of the SANDER program was modified to make it possible.

Initial conformation for each window of the umbrella sampling was taken from the TMD simulations performed in two directions, and the resulting histograms were combined to obtain the potential of mean force (PMF) of the transition pathway by using WHAM.<sup>26</sup> The same reference conformations for 3BJ5Z and 5BJ3Z used in the TMD simulations were taken to be the two reference conformations. The target  $\Delta\text{rmsds}$  selected for umbrella sampling windows ranged from  $-6.6$  to  $6.6$  Å with  $0.3$  Å intervals, leading to a total of 45 windows.

The overlapping windows, the windows for which umbrella sampling results obtained starting from the two TMD trajectories are combined in the PMF calculations, were determined based on the conformational similarity. More specifically, the windows with sufficient similarity to the midpoint of the transition that shared the following two key features were selected: extrusion of the bases of DC4, DG15, and DC14 and hydrogen bonding of the DC14 base with the backbone oxygen atoms in the same strand (see the Results and Discussion for structural details for the midpoint structure). Five windows of  $\Delta\text{rmsd}$ , from  $-0.6$  to  $-1.8$  Å, were chosen as a result. Two of the windows of  $\Delta\text{rmsd}$ ,  $0$  and  $-0.3$  Å, were not included because conformations within  $\Delta\text{rmsd} - 0.5$  Å were not reached in the second TMD due to thermal fluctuations.<sup>17</sup> The exact extent of the overlapping region does not change the qualitative results, as discussed in the Results and Discussion.

A strong force constant of  $2.71$  kcal/mol per atom was initially imposed to prevent sudden collapse of the initial conformations when velocities were randomly assigned and gradually reduced to  $0.110$  kcal/mol per atom during  $200$  ps of MD simulation under NVT condition. The total force constant exerted on the double helix,  $N k_U$ , was  $40$  kcal/mol because  $N = 396$ . This value of the force constant gave sufficient overlaps in the sampled  $\Delta\text{rmsd}$  values between adjacent windows. For each window NPT simulation was carried out for  $1.5$  ns, and the data for the latter  $1.2$  ns were subject to analysis.  $\Delta\text{rmsd}$  was recorded at every step of MD simulations while the full Cartesian coordinates were written at every  $1$  ps. All the analysis of trajectories and calculation of the geometric parameters of DNA were performed with the PTTRAJ program in AMBER9.

## Results and Discussion

**The Two End Points of the Transition, 3BJ5Z and 5BJ3Z, Are Locally Stable.** Since this is the first atomistic MD simulation study involving a B-Z junction, it is necessary to examine whether the proposed end points of the transition, 3BJ5Z and 5BJ3Z, are well described by the current molecular system and force field before investigating the pathway of the transition. We therefore carried out MD simulations of the two end point states before simulating the transition between the

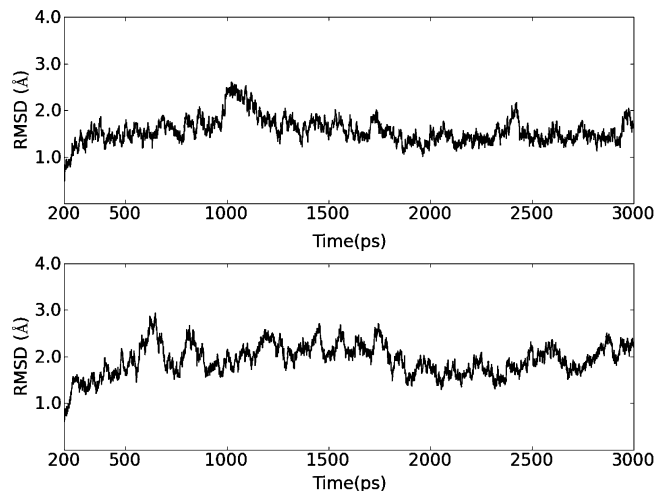


**Figure 3.** rmsds of the two states, 3BJ5Z (a) and 5BJ3Z (b), as a function of simulation time. rmsd here refers to the root-mean-square deviation of all heavy atoms including atoms of terminal nucleotides from the initial model constructed directly from the crystal structure.

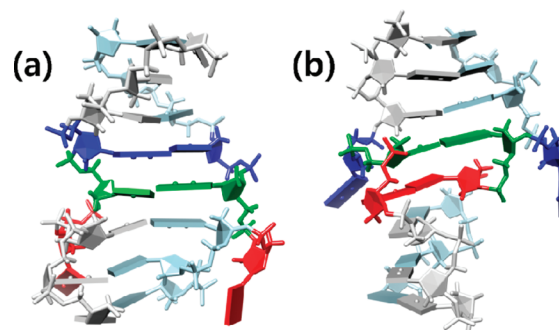


**Figure 4.** The last snapshots of the two 3 ns unconstrained molecular dynamics simulations of 5BJ3Z (a) and 3BJ5Z (b). The color code is the same as in Figure 2.

two states. It is of interest to see whether a DNA fragment of a GC-repeat with no Z-DNA binding protein forms a locally stable B-Z junction structure similar to the crystal structure.

We chose the nucleotide sequence, a GC repeat, different from that for which the crystal structure is known because (1) it enables us to compare our results with previous experiments and simulations regarding thermodynamics and kinetics of GC oligomers and (2) the symmetry of the poly-GC sequence allows us to draw the free energy difference between B-DNA and Z-DNA from the free energy difference between the two end points, 5BJ3Z and 3BJ5Z, if terminal effects are ignored.

Two NPT MD simulations with explicit water molecules were carried out for  $3$  ns after gradual heating for  $200$  ps at constant volume, as described in the Methods section. Both of the two “non-canonical” double-strand conformations, 3BJ5Z and 5BJ3Z, were stable for the whole period of the simulation time, in marked contrast to A-DNA, which undergoes a spontaneous transformation to B-DNA on the nanosecond time scale.<sup>34</sup> Figure 3 shows that both states remain stable, close to the initial structures constructed from the crystal structure, with rmsd below  $3$  Å. The structures of the last snapshot of the simulations are depicted in Figure 4, and it can be confirmed that they maintain similar junction structures to the crystal structure shown in Figure 1. B-Z junctions are expected to be stable for much longer periods than nanoseconds based on the observation that the B-Z transition occurs in the time scale of seconds to

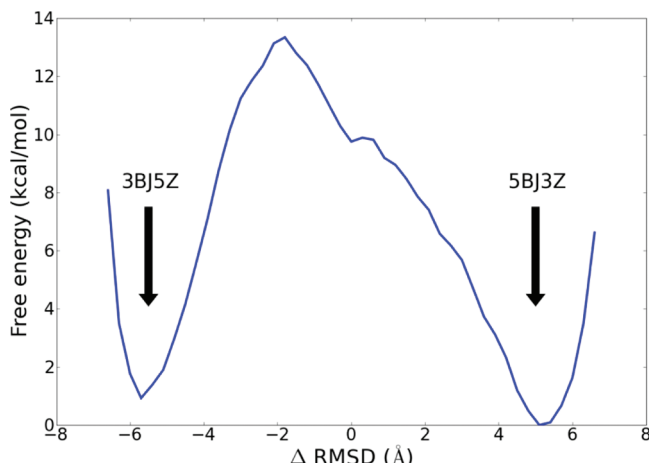


**Figure 5.** The potential of mean force of a dinucleotide progression of the B–Z junction with respect to the  $\Delta\text{Rmsd}$  coordinate. The region of positive  $\Delta\text{Rmsd}$  corresponds to a state closer to 5BJ3Z than 3BJ5Z. The free energy change caused by the junction movement is 0.93 kcal/mol. The location of the minimum free energy for 3BJ5Z is  $\Delta\text{Rmsd} = -5.7 \text{ \AA}$  and that for 5BJ3Z is  $5.1 \text{ \AA}$ . The transition state is located at  $\Delta\text{Rmsd} = -1.8 \text{ \AA}$ , and the height of the barrier for the transition from 5BJ3Z to 3BJ5Z is 13.3 kcal/mol.

minutes,<sup>6,35</sup> and the current simulation results are compatible with this fact.

The most distinguished conformational variations observed in the simulation trajectories were flexible rotations of the extruded bases and fluctuations of the terminal nucleotides. The standard deviations of the rotation angle of the glycosidic bond,  $\chi$ , for nucleotides that maintain a regular WC base pair in the simulation trajectories were in the range of 10.4–22.0° (terminal nucleotides are not included). Those for the extruded bases at the junctions, DC4 and DG15 of 5BJ3Z and DC6 and DG13 of 3BJ5Z, are in the range of 29.2–66.2°. This increased flexibility of the extruded bases is expected to play an important role in the B–Z transition by providing a low free energy barrier for reformation of the WC base pair with base-plane flipping.

Because the unconstrained MD simulations are not expected to lead to spontaneous transitions within typical simulation time scales, it is necessary to employ a technique to accelerate the transition. Here, we employed targeted molecular dynamics simulation and umbrella sampling, and the results are presented below.

**Free Energy Landscape for the B–Z Junction Propagation.** The potential of mean force (PMF) of the B–Z junction propagation obtained from the WHAM analysis of the umbrella sampling simulations along the  $\Delta\text{Rmsd}$  coordinate is shown in Figure 5. The existence of two pronounced free energy minima located toward the two end points is consistent with the fact that the unconstrained MD simulations showed considerable stability of the two end points of the transition. The free energy difference of the two minima, or the free energy of the junction propagation by two nucleotide blocks, is evaluated to be 0.93 kcal/mol. This value is in close agreement with the free energy of junction propagation obtained from the 2D-gel experiments on a GC-repeat sequence, 0.66 kcal/mol.<sup>8</sup> Other experimental studies on various Z-DNA forming sequences with CD spectroscopy<sup>36</sup> and a thermodynamic approach based on genomic information<sup>11</sup> showed that the free energy cost of junction propagation is generally less than 2 kcal/mol.

Convergence of the potential of mean force was checked by comparing the PMFs evaluated with ten equally divided subsets of umbrella sampling trajectories. Each subset therefore corre-

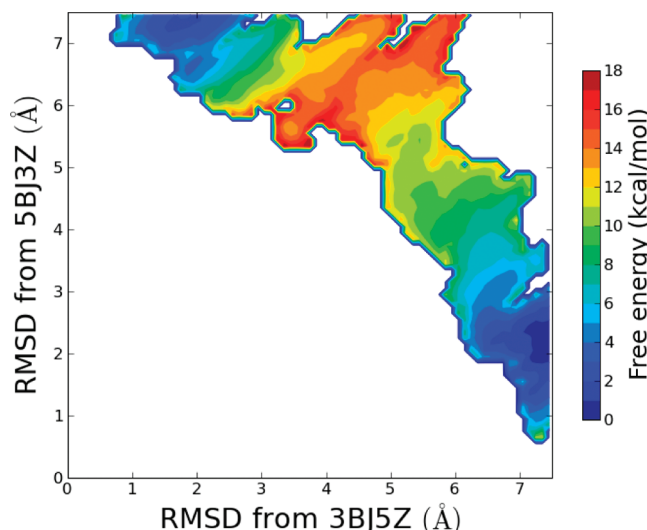


**Figure 6.** Two-dimensional potential of mean force of the B–Z junction translation by a dinucleotide unit. The global minimum of the PMF is located at  $2.35 \text{ \AA}$  from the 5BJ3Z and  $7.45 \text{ \AA}$  from the 3BJ5Z reference structure. The local minimum in the 3BJ5Z structure is located at  $7.35 \text{ \AA}$  from the 5BJ3Z and  $1.85 \text{ \AA}$  from the 3BJ5Z reference structure. The free energy difference between the two minima is 1.7 kcal/mol, and the height of the barrier of the transition from 5BJ3Z to 3BJ5Z is 14 kcal/mol.

sponds to 120 ps dynamics simulations of 45 windows. The standard deviations of the ten PMFs suggest that the result is precise to 1–1.5 kcal/mol. The result of this convergence test is illustrated in Figure 1 in the Supporting Information.

The free energy of the junction propagation can also be interpreted as the free energy difference between B-DNA and Z-DNA per dinucleotide-pair if the terminal effects due to the short length of the DNA fragments are ignored. The estimated free energy difference is then 0.47 kcal/mol per base pair.

The free energy barrier of the transition from 5BJ3Z to 3BJ5Z is estimated to be 13.3 kcal/mol from Figure 5. This value is comparable to the free energy barrier of the single-base flipping, estimated from previous umbrella sampling simulations, 10–20 kcal/mol.<sup>37,38</sup> This fact supports our hypothesis that the B–Z junction movement can be accomplished with a low free energy barrier comparable to that for a simple transition that involves only local conformational change.

The exact PMF can be affected by the exact extent of the overlapping region in our WHAM analysis. As explained in the Methods section, we selected the overlapping windows from the similarity of the structures to minimize noises from irrelevant structures. We have checked the effect of varying the overlapping region by changing the number of overlapping windows from 1 to 7. The sign of the free energy difference was reversed when 3 or fewer windows overlapped ( $-1.1$ ,  $-0.5$ , and  $-0.1$  kcal/mol for overlapping regions of  $\Delta\text{Rmsd} = -0.6 \text{ \AA}$ ,  $-0.6$  to  $-0.9 \text{ \AA}$ , and  $-0.6$  to  $-1.2 \text{ \AA}$ , respectively), but the magnitudes are very small. For overlapping regions of  $\Delta\text{Rmsd} = -0.6$  to  $-1.5 \text{ \AA}$ ,  $-0.6$  to  $-1.8 \text{ \AA}$ ,  $-0.6$  to  $-2.1 \text{ \AA}$ , and  $-0.6$  to  $-2.4 \text{ \AA}$ , the free energy differences were 0.2, 0.9, 1.7, and 2.3 kcal/mol, respectively. We selected the overlapping region  $-0.6$  to  $-1.8 \text{ \AA}$  because this region shares the maximal consistency among the ensembles of sampled structures, as explained in the Methods section. Deviations from this choice do not change the qualitative results or conclusions of this paper.

The potential of mean force (PMF) in the two-dimensional space of the two rmsd values from the two reference structures is also depicted in Figure 6. Although umbrella sampling was

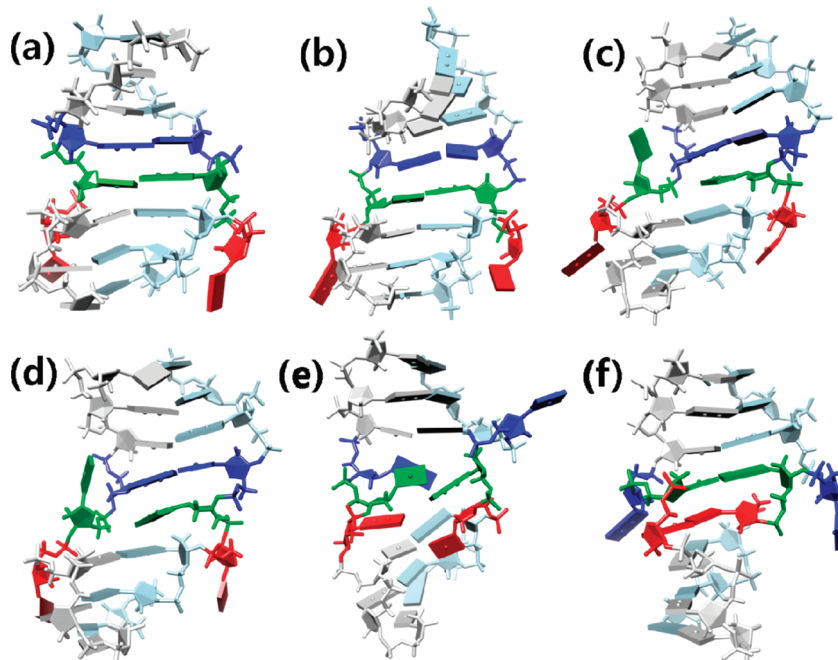


**Figure 7.** Trajectory of the junction translation, from 5BJ3Z to 3BJ5Z. The Z-DNA character increases from parts a to f. The color code for nucleotides is identical with that in Figure 2. Nucleotides undergoing large conformational changes are shown in red, green, and blue.

performed along the one-dimensional  $\Delta\text{rmsd}$  coordinate, intuition into a more detailed shape of the free energy surface can be obtained from the two-dimensional (2D) PMF. The 2D PMF illustrates that there is no additional local free energy minimum and that our conformational sampling covers a large part of the right-upper triangle region that is of physical interest. The free energy difference of 1.7 kcal/mol between the two minima and the free energy barrier of 14 kcal/mol qualitatively agree with those obtained from the WHAM analysis in the  $\Delta\text{rmsd}$  coordinate.

**Conformational Changes in the Transition Pathway.** Conformational changes involved in the B-Z junction movement have been investigated by analyzing the representative structures of the umbrella sampling windows instead of the TMD trajectories which are the initial structures for umbrella sampling. Umbrella sampling simulations were carried out with a much weaker restraining potential for a longer simulation time than the TMD simulations, allowing for more relaxation. The center of the largest cluster of the conformational ensemble of each umbrella sampling window was selected as the representative conformation of the window.

The representative structures of 6 windows ( $\Delta\text{rmsd} = 6.6, 2.7, -0.3, -0.6, -1.8$ , and  $-6.6 \text{ \AA}$ ) are depicted in Figure 7 in the order of increasing Z-DNA character, from 5BJ3Z to 3BJ5Z. Four characteristic features were observed in the trajectory: (1) a partial stretching and parallelization of the backbone near the junction, (2) extrusion of the cytosine base of DC14, which is in between the extruded bases of 5BJ3Z (DG15) and 3BJ5Z (DG13), (3) stacking interactions of the guanine base of DG5 with two neighboring guanines of DG13 and DG3 upon WC pair breaking due to DC14 extrusion, and (4) initiation of extruded base insertion by the formation of hydrogen bonds with neighboring bases. Details of these features are explained below.

In the initial stage of the junction movement from 5BJ3Z to 3BJ5Z, all nucleotides except for the extruded bases of the junction adopt near-canonical B-DNA or Z-DNA structures (see Figure 7a). The first distinctive conformational change observed

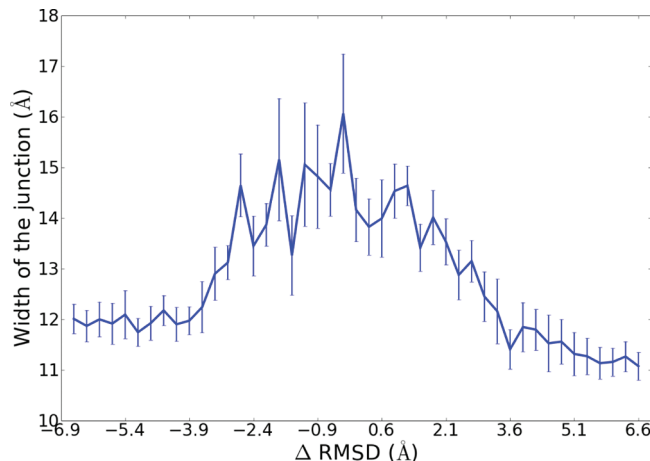


**Figure 8.** Changes in the width of the junction region during the reaction are illustrated with standard deviations represented by error bars. The width of the junction is defined as the average distance between the mass centers of the DG7-DC12 and DG3-DC16 pairs. The width decreases from  $12 \text{ \AA}$  to  $11 \text{ \AA}$  as the structure changes from 3BJ5Z to 5BJ3Z. This value coincides with the differences in the length of the helical pitch observed in crystal structures of B- and Z-DNA. During the transition, the width increases up to  $16 \text{ \AA}$ , indicating significant stretching of the DNA backbone.

for the transition is partial stretching and parallelization of the B-DNA backbone close to the extruded bases without breaking of any hydrogen bonds, as depicted in Figure 7b. Stretching near the junction was more closely examined by measuring the distance,  $d_{\text{junc}}$ , between the centers of mass of the DG7-DC12 and DG3-DC16 pairs whose WC pairing is maintained throughout the transition. The average distance,  $\langle d_{\text{junc}} \rangle$ , at each umbrella sampling window is plotted in Figure 8. The average distance for 5BJ3Z and 3BJ5Z ( $\Delta\text{rmsd} = -6.6$  and  $6.6 \text{ \AA}$ ) is  $11$  and  $12 \text{ \AA}$ , respectively, consistent with the fact that Z-DNA is longer than B-DNA by  $0.5 \text{ \AA}$  per base pair. During the transition the width increases up to  $16 \text{ \AA}$  at  $\Delta\text{rmsd} = 0.0 \text{ \AA}$ . This stretching is interpreted as facilitating the base rotation necessary for the B-Z transition, as described below in more detail. A stretched

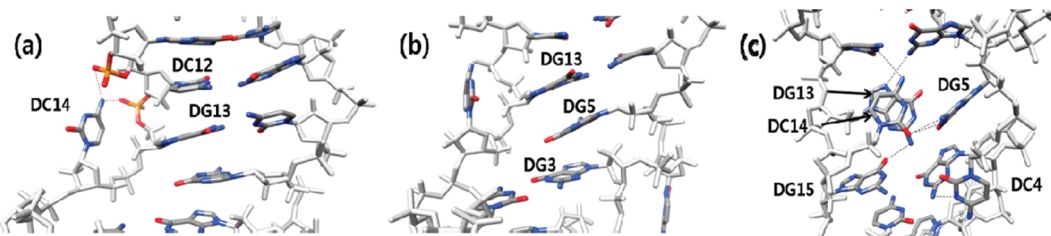


**Figure 9.** Three key structural changes observed during the transition. (a) The base of DC14 located in between the extruded pairs in the end points of the transition is partially extruded and forms hydrogen bonds with phosphate groups in the same strand. (b) After DC14 is flipped out, the orphan nucleotide, DG5, is stabilized by stacking interactions with adjacent guanine bases of DG13 and DG3. (c) DC14 moves in by making hydrogen bonds with DG5 and stacking interaction with DG13. DG15 and DC4 also move in by forming hydrogen bonds with neighboring bases before forming a WC pair.

intermediate model was also suggested in previous studies,<sup>15,18</sup> although in the different context of a concerted transition that involves the entire DNA backbone. The current result could be tested by single-molecule FRET experiments in the future.

After straightening of the backbone, the base of DC14 was observed to swing out, as can be seen in Figure 7c. Note that DC14 is not extruded in the initial or final conformations of the transition but is located between the bases that are extruded. The energy loss due to breaking of the WC pairing between DC14 and DG5 is compensated for by the hydrogen bonding with the phosphate groups of DG13 and DC12 in the same strand, as shown in more detail in Figure 9a. Similar backbone-base hydrogen bonding was observed in a simulation of the base flipping reaction.<sup>39</sup> The base plane of DC14 would be rotated more easily if the base is extruded than if it maintains a WC pair. The base extrusion also provides more space inside the helix for rotation of the base plane of DG5.

Upon extrusion of DC14, DG5, which lost the hydrogen bonding partner, and DG13, which lost a stacking partner, make stabilizing stacking interactions, as shown in Figure 7d. The triplet stacking of DG13, DG5, and DG3 shown in Figure 9b accompanies movement of DG5 toward the space originally occupied by DC14, which helps to establish the Z-DNA-like backbone structure.

In the previous TMD simulation study on the B-Z transition,<sup>18</sup> it was discussed that the energetic cost caused by the loss of WC pairing is compensated for by an increase in DNA–water hydrogen bonds. A similar trend was observed in our simulation, although the change in the number of hydrogen bonds is much smaller here probably because only local changes are involved. About three intra-DNA hydrogen bonds are lost near the transition state compared to the end points, and about ten DNA–water interactions are newly formed, as shown in Figure 2 in the Supporting Information.

Finally, the DC6-DG13 pair is broken, and the DC4-DG15 pair is formed completing the junction movement by two nucleotides, as shown in Figure 7e,f. When DC6 is flipped out, DG13 makes a stacking interaction with DC14, which moves back toward DG5 forming hydrogen bonds, as shown in more detail in Figure 9c. The stacking bases of DG13 and DC14 are oriented vertically to other bases, indicating that base rotation of DC14 is on the way. WC pair formation of the extruded bases of DC4 and DG15 occurs at the same time, initiated by hydrogen bond formation with neighboring bases in the same strand, DG3 and DC14, respectively.

To confirm the maintenance of the canonical B-DNA or Z-DNA structure at each end of the DNA chain throughout the transition, various helical parameters were monitored. The helical twist (rotation of successive base pairs around the helical axis) is one of the most distinctive parameters that discriminate

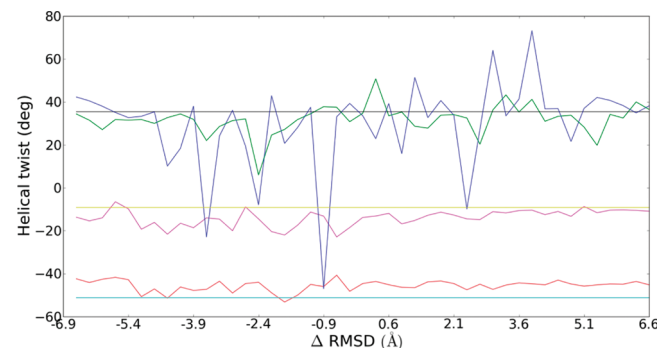


**Figure 10.** The helical twist angles of the two base-pair steps at each end of DNA are plotted along the reaction coordinate  $\Delta\text{rmsd}$ . The helical twist angles for the two steps of the B-DNA end (shown in blue and green) fluctuate around the canonical value  $36^\circ$ . Those for the CpG and GpC steps of the Z-DNA end (shown in magenta and red) stay close to the canonical values,  $-9^\circ$  and  $-51^\circ$ , respectively.

Z-DNA from B-DNA because the sign of the angle is reversed. We calculated the helical twist for the two base-pair steps (which involve three base pairs) at each end of the DNA from the average structure of each umbrella sampling window. Changes in the helical twist during the transition are plotted in Figure 10. It can be confirmed that the helical twist angles at both ends of the DNA remain close to the canonical values ( $36^\circ$  for B-DNA and  $-9^\circ$  and  $-51^\circ$  for the CpG and GpC steps of Z-DNA, respectively). The large fluctuation in the helical twist of the B-DNA end at  $\Delta\text{rmsd} = -0.9 \text{ \AA}$  is due to breaking of Watson–Crick base-pairing at the terminal, which is caused by the large elongation of the double strand during the transition.

The above trajectory sheds new light on the mechanism of the B-Z transition and conformational diversities of DNA. According to our simulations, base pair plane flipping and backbone handedness change occurs simultaneously. The backbone is stretched locally and parallelized before winding in the opposite direction. The way base pair plane flipping is accomplished is delicate. The base planes of the extruded bases can be flipped easily. The smaller cytosine base next to the extruded pair is partially extruded and flipped, and its WC partner guanine base rotates inside the helix in our simulation. These observations lead to the interpretation that the B-Z transition is facilitated by the intrinsic structural property of the B-Z junction that compartmentalizes the DNA structure into a local transition region and the remaining canonical regions, avoiding the large free energy cost involving conformational change of the entire Z- or B-DNA.

**Potential of Mean Force for Internal Coordinates: Glycosidic Bond Torsion Angles and Sugar Pucker Angles.** The glycosidic bond torsion angle (denoted by  $\chi$ ) and the sugar pucker angle (represented by the pseudorotation angle  $P$ ) are

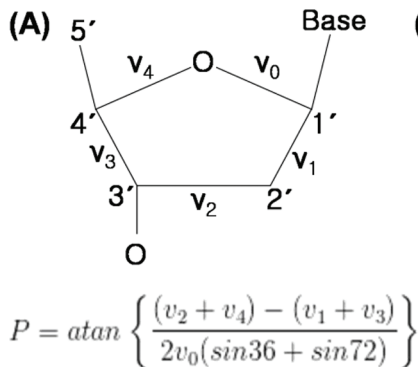


**Figure 11.** The axes of rotation for the five torsion angles,  $v_0$ – $v_4$ , of a five-membered furanose ring are indicated, and the pseudorotation angle  $P$  is defined in terms of the five angles in part A. Changes in the five torsion angles during a cycle of  $P$ ,  $0 \leq P \leq 360^\circ$ , are plotted in part B. The  $\chi$  angle, defined as  $O4'-C1'-N9-C4$  for purine and as  $O4'-C1'-N1-C2$  for pyrimidine, and the *anti* and *syn* conformations are illustrated in part C.

two of the main indicators of DNA conformational change. We therefore calculated the potential of mean forces along  $\chi$  and  $P$  angles of individual nucleotides to examine how transitions of these angles are accomplished in a more quantitative manner. See Figure 11 for the definition of  $\chi$  and  $P$ .

Since we did not impose direct restraints on these variables during umbrella sampling, sufficient sampling is not guaranteed, especially at higher free energy regions; however, the rough nature of the PMFs still can be examined. Five nucleotide pairs are considered: DC8-DG11 that remains in the B-DNA conformation throughout the transition, DC2-DG17 that remains in the Z-DNA conformation, DC6-DG13 that takes a B-like conformation in 5BJ3Z and becomes extruded in 3BJ5Z, DG4-DC15 that is extruded in 5BJ3Z and becomes a Z-like conformation in 3BJ5Z, and DG5-DC14 that changes from a B-like to a Z-like conformation. The base plane of DG5-DC14 is flipped over in the course of the transition.

**A. Potential of Mean Force for Glycosidic Bond Torsion Angles.** The glycosidic bond torsion angle  $\chi$  is the dihedral angle that determines orientation of the base relative to the sugar, defined as the  $O4'-C1'-N9-C4$  dihedral angle for purine nucleotides and the  $O4'-C1'-N1-C2$  angle for pyrimidine. According to crystallographic studies, two states, *syn* ( $\chi \approx +45^\circ$ ) and *anti* ( $\chi \approx -135^\circ$ ), are preferred. Every nucleotide in B- or A-DNA and pyrimidine nucleotides in Z-DNA adopt the *anti* conformation, but purine nucleotides in Z-DNA take the *syn* conformation.

The PMFs for the  $\chi$  angles of the nucleotides that remain in the B- or Z-DNA conformation show a single minima, as expected, in the *anti* conformation for DC8 and DG11 that are in B-DNA (see Figure 12e) and in the *anti* for DC2 and *syn* for DG17 that are in Z-DNA (see Figure 12a). The locations of the minima are summarized in Table 1 in the Supporting Information.

The PMFs of nucleotides that form parts of the B-Z junction by being extruded out have more complex shapes (see Figure 12b,d). The PMFs show mixed features of single minima for canonical B- or Z-DNA and broad minima for less restrained extruded nucleotides, spanning the high-*anti* region (between *anti* and *syn*). The free energy barriers between the minima are small (1–4 kcal/mol), indicating that rotation about the glycosidic bonds for these nucleotides is relatively easily accomplished during the junction movement. The free energy difference between the minima and the free energy barriers for the transition between the minima are also summarized in Table 1 (Supporting Information).

The PMFs of nucleotides that undergo transition from B-like to Z-like conformations, shown in Figure 12c, also have multiple

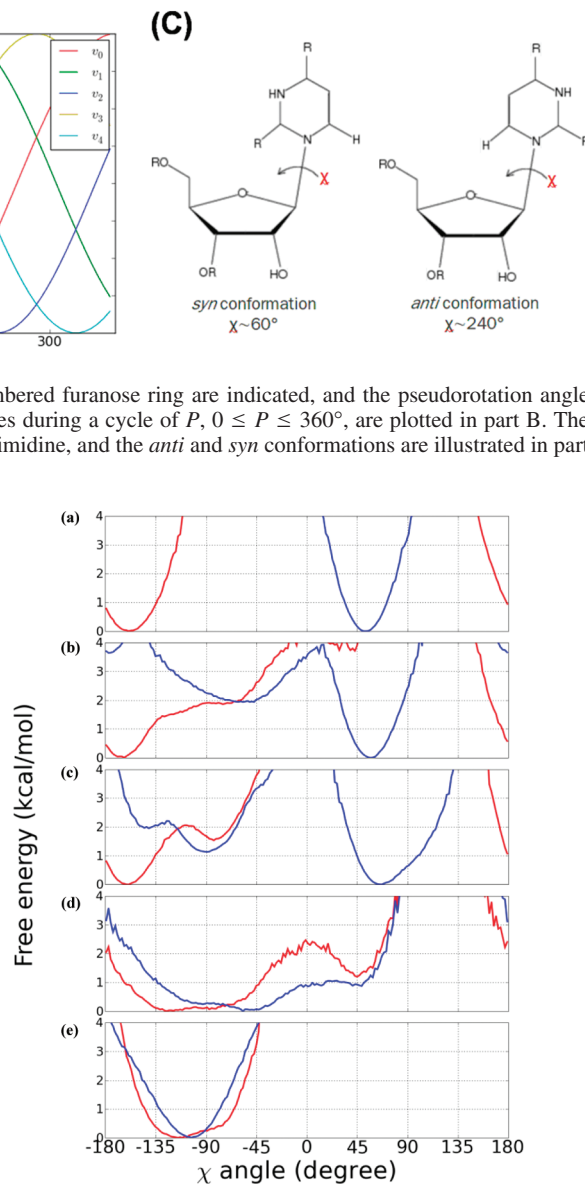


**Figure 12.** The PMFs of the glycosidic bonds of nucleotides located in five different environments: (a) Z-DNA (DC2-DG17), (b) Z-DNA and extruded bases (DC4-DG15), (c) B-DNA and Z-DNA (DG5-DC14), (d) B-DNA and extruded bases (DC6-DG13), and (e) B-DNA (DC8-DG11). Blue and red lines correspond to the PMFs for guanine and cytosine nucleotides, respectively. In the two canonical cases (a and e), each nucleotide has only one free energy minimum. The PMFs are plotted with a cutoff at 4 kcal/mol because of insufficient sampling beyond these regions.

minima and population in the high-*anti* region, but with higher free energy barriers. Base flipping for DG5 involves the highest free energy barrier (>4 kcal/mol) among different  $\chi$  angles.

It can be now concluded that the conformation of the B-Z junction enhances flexibilities of the extruded bases and lowers the free energy barrier for base flipping considerably. It has also been found that the high-*anti* conformation plays the role of an intermediate between the canonical *syn* and *anti* conformations in the B-Z transition.

**B. Potential of Mean Force for Sugar Pucker Angles.** The pseudorotation phase angle  $P$  is typically used to describe the sugar pucker state.<sup>40</sup> A deoxyribose ring is known to have two energy minimum conformations, C2'-endo ( $P \approx 180^\circ$ ) and C3'-endo ( $P \approx 10^\circ$ ). B-DNA adopts C2'-endo, while Z-DNA adopts C2'-endo for pyrimidine and C3'-endo for purine nucleotides.

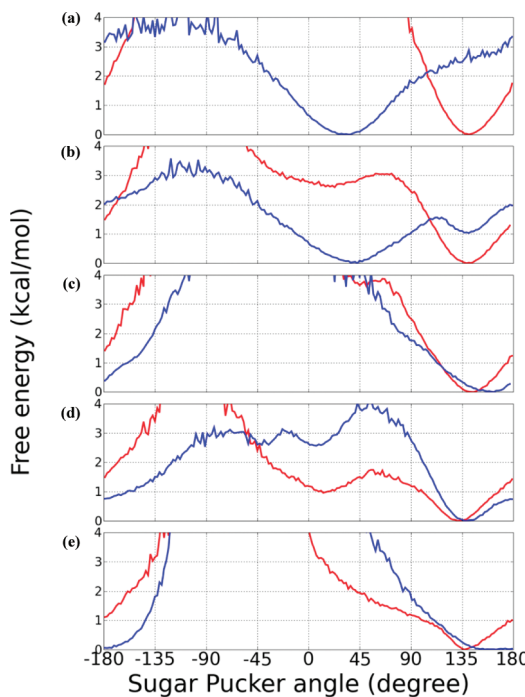


**Figure 13.** The PMFs of sugar puckers located in five different environments: (a) Z-DNA (DC2-DG17), (b) Z-DNA and extruded bases (DC4-DG15), (c) B-DNA and Z-DNA (DG5-DC14), (d) B-DNA and extruded bases (DC6-DG13), and (e) B-DNA (DC8-DG11). Blue lines represent guanine bases and red lines cytosine bases. The PMFs are plotted with a cutoff at 4 kcal/mol because of insufficient sampling beyond these regions.

The PMFs for the pseudorotation angles of the nucleotides that remain in the B- or Z-DNA conformation show single minima at canonical values, as expected, at C2'-endo for DC8 and DG11 that are in B-DNA (see Figure 13e) and C2'-endo for DC2 and C3'-endo for DG17 that are in Z-DNA (see Figure 13a).

The PMFs of nucleotides that form parts of the B-Z junction by being extruded out show secondary minima, as can be seen from Figure 13b,d. The free energy barriers between the minima are low (1–4 kcal/mol), as is the case for the  $\chi$  angle change, indicating that the sugar pucker states for these nucleotides can also be easily interconverted during the junction movement. The locations of the minima, the free energy difference, and the transition barrier between the minima are summarized in Table 2 (Supporting Information).

The PMFs of nucleotides that undergo transition from B-like to Z-like conformations have only single minima, as can be seen from Figure 13c, although the  $P$  angle of DG5 may be expected to have an additional minimum at C3'-endo conformation corresponding to the Z-DNA conformation. We think that this is because DG5 is located right next to the extruded nucleotides and deviates from both B- and Z-DNA conformation. Nucleotides next to the extruded ones do not exactly correspond to the canonical B- or Z-DNA in their crystal structure.<sup>14</sup> However, the base plane for DG5-DC14 was confirmed to be flipped over during the transition.

The flexibility of nucleotides observed in the above PMFs reiterates that the B-Z junction movement is facilitated by the flexibility of the extruded nucleotides. It has been observed that cytosine nucleotide is more flexible than guanine in the transition probably because of the smaller size of the base and the weaker  $\pi-\pi$  stacking interaction.

## Conclusion

Interconversion between the canonical, right-handed B-DNA and the noncanonical, left-handed Z-DNA is a fascinating structural change of DNA by itself and also has biological importance, being involved in gene expression and gene processing events. Elucidation of the mechanism of the B-Z transition is of great interest because it can deepen our understanding of the diversity and flexibility of the DNA structures and also provide useful information for development of therapeutic treatments for Z-DNA-related diseases.

Our proposal for the B-Z junction movement as an elementary step for the B-Z transition was inspired by the surprisingly simple crystal structure for the “static” B-Z junction stabilized by specific binding of Z-DNA binding proteins. Here we have shown that it is highly probable that such a junction can also be involved in the “dynamic” B-Z transition that is not assisted by proteins.

The proposed mechanism, sequential propagation of a B-Z junction, applies directly to situations in which B-Z junctions already exist, for example upon unbinding of Z-DNA binding proteins from the Z-DNA regions or upon release of negative superhelical stress in DNA regions containing Z-DNA. The mechanism can also be conceived to occur in the Z-DNA formation due to introduction of negative superhelical stress or an increase in salt concentration. However, the current study does not deal with nucleation of B-Z junctions.

Our simulation shows that the stepwise propagation of a B-Z junction provides a much lower free energy barrier than the concerted transformation of the entire helix observed in previous molecular simulations. The free energy barrier is lower because perturbation to the canonical DNA structure can be limited to only a few nucleotides by the presence of the B-Z junction. Such a local perturbation is possible because the B-Z junction can effectively compartmentalize the two incompatible DNA structures, B-DNA and Z-DNA, with a single extruded base pair. However, the concerted transformations observed in previous simulations may be involved in the nucleation of B-Z junctions, which would require a higher free energy barrier.

The current simulations still have the limitations of typical TMD simulations, although we tried to avoid them by carefully designing the end points of the transition and by performing bidirectional TMD and extensive umbrella sampling simulations. We expect that more thorough sampling with those methods that make use of the minimum action principle<sup>41–44</sup> may help to locate the transition pathway more precisely. However, the general discussion regarding the stepwise transition versus concerted transition would still be valid.

**Acknowledgment.** K.K.K. acknowledges the support by the National Research Laboratory Program (NRL-2006-02287). We also would like to acknowledge the support from the KISTI Supercomputing Center.

**Supporting Information Available:** Two supplementary tables giving a summary of the potential of mean forces of glycosidic bonds and of sugar pockers and two supplementary figures showing a convergence test of the potential of mean force in the  $\Delta\text{rmsd}$  reaction coordinate and the average number of intra-DNA hydrogen bonds. This material is available free of charge via the Internet at <http://pubs.acs.org>.

## References and Notes

- (1) Andrew, H. J. W.; Quigley, G. J.; Kolpak, F. J.; Crawford, J. L.; van Boom, J. H.; van der Marel, G.; Rich, A. *Nature* **1979**, 282, 680.

- (2) Schroth, G.; Chou, P.; Ho, P. *J. Biol. Chem.* **1992**, *267*, 11846.  
(3) Oh, D.; Kim, Y.; Rich, A. *Proc. Natl. Acad. Sci. U.S.A.* **2002**, *99*, 16666.  
(4) Rich, A.; Zhang, S. *Nat. Rev. Genet.* **2003**, *4*, 566.  
(5) Wang, G.; Christensen, L.; Vasquez, K. *Proc. Natl. Acad. Sci. U.S.A.* **2006**, *103*, 2677.  
(6) Pohl, F. M.; Jovin, T. M. *J. Mol. Biol.* **1972**, *67*, 375.  
(7) Herbert, A.; Lowenhaupt, K.; Spitzner, J.; Rich, A. *Proc. Natl. Acad. Sci. U.S.A.* **1995**, *92*, 7550.  
(8) Peck, L. J.; Wang, J. C. *Proc. Natl. Acad. Sci. U.S.A.* **1983**, *80*, 6206.  
(9) Goto, S. *Biopolymers* **1984**, *23*, 2211.  
(10) Ho, P.; Ellison, M.; Quigley, G.; Rich, A. *EMBO J.* **1986**, *5*, 2737.  
(11) Ho, P. *Proc. Natl. Acad. Sci. U.S.A.* **1994**, *91*, 9549.  
(12) Harvey, S. *Nucleic Acids Res.* **1983**, *11*, 4867.  
(13) Saenger, W.; Heinemann, U. *FEBS Lett.* **1989**, *257*, 223.  
(14) Ha, S. C.; Lowenhaupt, K.; Rich, A.; Kim, Y. G.; Kim, K. K. *Nature* **2005**, *437*, 1183.  
(15) Lim, W.; Feng, Y. *Biophys. J.* **2005**, *88*, 1593.  
(16) Elber, R.; Ghosh, A.; Cardenas, A. *Acc. Chem. Res.* **2002**, *35*, 396.  
(17) Schlitter, J.; Engels, M.; Kruger, P.; Jacoby, E.; Wollmer, A. *Mol. Simul.* **1993**, *10*, 291.  
(18) Kastenholz, M.; Schwartz, T.; Hunenberger, P. *Biophys. J.* **2006**, *91*, 2976.  
(19) Dai, Z.; Thomas, G.; Everts, E.; Petricolas, W. *Biochemistry* **1989**, *28*, 6991.  
(20) Sheardy, R.; Winkle, S. *Biochemistry* **1989**, *28*, 720.  
(21) Torrie, G.; Valleau, J. *J. Comput. Phys.* **1977**, *23*, 187.  
(22) Banavali, N.; Roux, B. *J. Am. Chem. Soc.* **2005**, *127*, 6866.  
(23) Kumar, S.; Rosenberg, J.; Bouzida, D.; Swendsen, R.; Kollman, P. *J. Comput. Chem.* **1992**, *13*, 1011.  
(24) Wang, A.; Hakoshima, T.; van der Marel, G.; van Boom, J.; Rich, A. *Cell* **1984**, *37*, 321.  
(25) Schroth, G.; Kagawa, T.; Ho, P. *Biochemistry* **1993**, *32*, 13381.  
(26) Eichman, B.; Schroth, G.; Basham, B.; Ho, P. *Nucleic Acids Res.* **1999**, *27*, 543.  
(27) Ha, S.; Choi, J.; Hwang, H.; Rich, A.; Kim, Y.; Kim, K. *Nucleic Acids Res.* **2009**, *37*, 629.  
(28) Cornell, W.; Cieplak, P.; Bayly, C.; Gould, I.; Merz, K.; Ferguson, D.; Spellmeyer, D.; Fox, T.; Caldwell, J.; Kollman, P. *J. Am. Chem. Soc.* **1995**, *117*, 5179.  
(29) Cheatham, T.; Cieplak, P.; Kollman, P. *J. Biomol. Struct. Dyn.* **1999**, *16*, 845.  
(30) Case, D.; Darden, T.; Cheatham, T., III; Simmerling, C.; Wang, J.; Duke, R.; Luo, R.; Merz, K.; Pearlman, D.; Crowley, M. *AMBER9*; University of California: San Francisco, 2006.  
(31) Jorgensen, W.; Chandrasekhar, J.; Madura, J.; Impey, R.; Klein, M. *J. Chem. Phys.* **1983**, *79*, 926.  
(32) Darden, T.; York, D.; Pedersen, L. *J. Chem. Phys.* **1993**, *98*, 10089.  
(33) Ryckaert, J.; Ciccotti, G.; Berendsen, H. *J. Comput. Chem.* **1977**, *23*, 327.  
(34) Cheatham, T., III; Kollman, P. *J. Mol. Biol.* **1996**, *259*, 434.  
(35) Brown, B.; Lowenhaupt, K.; Wilbert, C.; Hanlon, E.; Rich, A. *Proc. Natl. Acad. Sci. U.S.A.* **2000**, *97*, 13532.  
(36) Sheardy, R. D.; Suh, D.; Kurzinsky, R.; Doktycz, M. J.; Benight, A. S.; Chaires, J. B. *J. Mol. Biol.* **1993**, *231*, 475.  
(37) Banavali, N.; MacKerell, A. *J. Mol. Biol.* **2002**, *319*, 141.  
(38) Giudice, E.; Varnai, P.; Lavery, R. *Nucleic Acids Res.* **2003**, *31*, 1434.  
(39) Bouvier, B.; Grubmuller, H. *Biophys. J.* **2007**, *93*, 770.  
(40) Saenger, W. *Principles of nucleic acid structure*; Springer-Verlag: New York, 1984.  
(41) Czerninski, R.; Elber, R. *J. Chem. Phys.* **1990**, *92*, 5580.  
(42) Henkelman, G.; Uberuaga, B.; Jonsson, H. *J. Chem. Phys.* **2000**, *113*, 9901.  
(43) Passerone, D.; Parrinello, M. *Phys. Rev. Lett.* **2001**, *87*, 108302.  
(44) Lee Woodcock, H.; Hodosek, M.; Sherwood, P.; Lee, Y.; Schaefer, H., III; Brooks, B. *Theor. Chem. Acc.* **2003**, *109*, 140.

JP103419T